RSC Advances

ROYAL SOCIETY OF CHEMISTRY

www.rsc.org/advances

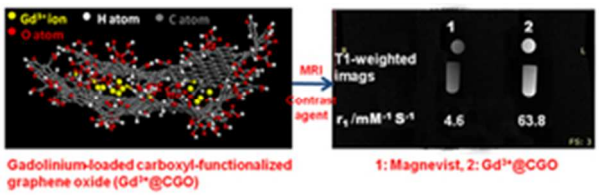

A facile synthetic strategy which leads to a high performance Gd3+ based MRI contrast agent (Gd3+@CGO) is developed using graphene oxide as a nanocarrier.
25x8mm (300 x 300 DPI)

RSC Advances

RSCPublishing

ARTICLE

Easy preparation of a MRI contrast agent with high longitudinal relaxivity based on gadolinium ions-loaded graphene oxide

Cite this: DOI: 10.1039/xoxxoooooox

Received ooth January 20xx,
Accepted ooth January 20xx

DOI: 10.1039/xoxxoooooox

www.rsc.org/

Xianyan Ren,[a,b] Xinli Jing,[a] Lihua Liu,[c] Liping Guo,[c] Ming Zhang,[c] and Yu Li [a]*

As far as the longitudinal relaxivity (r_1) to be concerned, gadolinium ions (Gd^{3+})-based MRI contrast modified by traditional carriers seem to be not far superior to the clinically used Magnevist. In this study, a kind of MRI contrast agent (Gd^{3+}@CGO) possessing a significantly high r_1 value was easily prepared using carboxyl-functionalized graphene oxide (CGO) as a nanocarrier to interact with $GdCl_3 \cdot 6H_2O$ directly. With the content of Gd^{3+} loaded on CGO of 2.8 wt%, the prepared Gd^{3+}@CGO shows good dispersibility in water and possesses r_1 of 63.8 $mM^{-1} S^{-1}$, which is 14 times higher than that of Magnevist. It is exciting that Gd^{3+} anchored on CGO remains stable at least for 1 year, probably relying on the electrostatic adsorption and physical encapsulation effect of CGO to Gd^{3+}.

1. Introduction

The clinical success of magnetic resonance imaging (MRI), a powerful noninvasive diagnostic modality, has fuelled an interest in techniques to prepare efficient contrast agents. Superparamagnetic iron oxide nanoparticles have attracted enormous attention in recent years due to their nontoxicity and cytocompatibility,[1] whereas the dark contrast of which restrains its clinical use. In contrary, gadolinium ions (Gd^{3+}) are characteristic of accelerating the longitudinal relaxivity (r_1) and therefore exhibiting bright contrast, which have been clinically used widely through coordination to polydentate chelator, e.g., the diethylene triamine pentacetic acid (DTPA) and diethylene triamine tetraacetic acid (DTTA). However, these low-molecular weight Gd^{3+} complexes are not ideal for application in many cases including cardiovascular and cancer imaging due to their shortages such as weak signal of contrast enhancement and rapid extravasating from the vasculature.[2] Much research has been done to improve MRI contrast enhancement by incorporating Gd^{3+} into various carriers such as polyamidoamine dendrimers,[3] quantum dots[4] and silica nanoparticles,[5] where complicated reactions are required to introduce DTPA or DTTA to coordinate Gd^{3+}.[6] The Gd^{3+}-loaded nanomaterials prepared through these methods display r_1 values ranging from 4.1 to 28.8 $mM^{-1} S^{-1}$, which actually are not remarkable compared with clinical Magnevist MRI contrast agent (r_1=3.4~4.1 $mM^{-1} S^{-1}$).

In virtue of the nano cavity, fullerenes and carbon nanotubes with good biocompatibility have been widely used as nanoplatforms for constructing high performance endohedral gadofullerene and gadonanotube based MRI contrast agents. Gd@C82[7] and Gd@C60[8] can be categorized into the first generation of gadofullerenes. Later on, $Gd@C60[C(COOH)_2]_{20}$ (r_1=4.6 $mM^{-1} S^{-1}$)[9] and $Gd_3N@C80[DiPEG5000(OH)_x]$ (r_1=143 $mM^{-1} S^{-1}$) with improved water solubility were developed.[10] Unfortunately, yields of these water-soluble gadofullerenes were low. Using current arc evaporation method, Zhang obtained two kinds of water-soluble gadofullerenes [$Sc_2GdN@C80O_{12}(OH)_{26}$, $ScGd_2N@C80O_{12}(OH)_{26}$] with high yield.[11] Nevertheless, gadofullerenes obtained in this way only show ordinary r_1 values (20.7 $mM^{-1} S^{-1}$ and 17.6 $mM^{-1} S^{-1}$, respectively) compared with Magnevist. Carbon nanotubes can also be used to encapsulate Gd^{3+} and lead to high performance MRI contrast agents. Wilson prepared superparamagnetic nanotubes with high r_1 value of 170 $mM^{-1} S^{-1}$ before hydrophilic modification, where Gd^{3+} clusters were loaded and confined by soaking and sonicating single-walled carbon nanotubes in $GdCl_3$ aqueous solution.[12] Generally speaking, Gd^{3+} ions are loaded into fullerenes and carbon nanotubes merely through a physical encapsulation effect.

In comparison with fullerenes and carbon nanotubes, the graphene oxide (GO) has significant advantages such as low cost and better water dispersibility benefitted from its abundant hydrophilic oxygen-containing groups,[13, 14] which make GO an attractive nanocarrier for MRI contrast agent. Furthermore, carboxyl-functionalized GO (CGO) possessing more carboxyl groups can show improved water solubility,[15] which was usually prepared by converting hydroxyl and epoxy groups of GO into carboxyl groups. These carboxyl groups can participate in esterification, amidation and coordination reactions,[16] thus broad the potential for functionalization of GO. Nevertheless, there are only a few reports about GO or CGO

used as a nanocarrier for Gd^{3+} based MRI contrast agents. Shen and his coworkers are the first ones who obtained a MRI contrast agent using CGO as a nanocarrier through electrostatic adsorption of Gd^{3+}-DTPA chloride on CGO sheets. However, in this case, Gd^{3+} ions were adsorbed on CGO enduring complicated reactions and still rely on DTPA, and the r_1 value of the product was not reported by the author.[17] Recently, an interesting finding was reported, i.e., carboxyphenylated graphene nanoribbons can be used as ligands to chelate Gd^{3+} and prepare high performance T_1-weighted MRI contrast agent.[18] However, the size of these nanoribbons was too large to ensure good biocompatibility[19], which was 125-280 nm, 7-15 nm and up to 20 mm in width, thickness, and length, respectively.

In this study, we develop an easy method to prepare high performance Gd^{3+}-based MRI contrast agents employing CGO as a nanocarrier without the assistance of polydentate chelator, i.e., DTPA or DTTA. The CGO is used without further treatment. GO sheets with lateral size of c.a. 200 nm are prepared and further carboxylated to form CGO by chloroacetic acid.

2. Experimental

2.1. Preparation of GO

GO was prepared from purified flake graphite (200 mesh) by a modified Hummers' method. Briefly, flake graphite (1 g) was mixed with concentrated H_2SO_4 (98 wt%, 33 mL) and $NaNO_3$ (0.5 g) at 0 ^oC for 20 min in an ice bath. Potassium permanganate (3 g) was added gradually with stirring while keeping the temperature of the mixture below 5 ^oC. Then the ice bath was removed and the mixture was stirred at 35 ^oC for 5 days. Finally, deionised water of 45 mL was added slowly and the temperature was kept at 98 ^oC for 2 h, followed by the addition of H_2O_2 (6 mL, 30 wt% aqueous solution) at 60 ^oC. In order to remove the ions of oxidant and other inorganic impurity, the resultant mixture was purified according to the protocol proposed by Zhang, L., *et al.* [20]

2.2. Preparation of CGO

The dried GO (100mg) powders were dispersed into deionised water (100 mL) and sonicated for 2 h to give a transparent solution. Sodium hydroxide (6g) and chloroacetic acid ($ClCH_2COOH$) (5g) were added to the GO solution and sonicated for 2 h under a temperature of 35 ^oC to convert the epoxy and hydroxyl groups of GO to carboxyl groups, giving CGO. The resulting CGO solution was purified by repeated rinsing and centrifugation until the product was totally dispersed in deionised water. As control, GO was treated through the same procedure mentioned above but with the absence of $ClCH_2COOH$, and the product was named as rGO.

2.3. Preparation of Gd^{3+}@CGO

Hexahydrate gadolinium chloride ($GdCl_3{\cdot}6H_2O$) was dissolved in deionised water to make a solution with a concentration of 1mg mL^{-1}. Then the $GdCl_3{\cdot}6H_2O$ solution of 4 mL was added dropwise into 50mL of CGO dispersion (1mg mL^{-1}) with stirring. After reaction duration of 12 h at a temperature approximately of 35 ^oC and a pH value of 6.5, the reaction mixture was precipitated with saturated NaCl aqueous solution. The supernatant was collected for following testing, and the precipitate was repeatedly centrifugated and washed with deionised water for three times, which was finally dried in vacuum oven at 50 ^oC to produce pure Gd^{3+}@CGO. As a comparison, $GdCl_3{\cdot}6H_2O$ aqueous solution of the same volume ratio was added to GO and rGO solution, respectively, experiencing the same reaction process as above.

A uniform powder mixture (Mx) containing Gd^{3+} of 2.8 wt% was prepared by well grinding CGO and $GdCl_3{\cdot}6H_2O$ together in an agate mortar.

2.4. Characterization methods

Two kinds of tests were performed to monitor whether Gd^{3+} ions from $GdCl_3{\cdot}6H_2O$ were all anchored on CGO stably after reaction. On the one hand, the collected supernatant was tested by xylenol orange and inductively coupled plasma optical emission spectrometer (ICP-OES, Varian 715). On the other hand, the reaction mixture of CGO with $GdCl_3{\cdot}6H_2O$ (after reaction of 12 h) was dialyzed against deionised water through a 500 D dialysis bag for 1 h, 5 h, 12 h and 24 h, respectively, and the Gd^{3+} concentration in these dialysates were tested by ICP-OES.

The interaction between Gd^{3+} and CGO was studied according to Zeta potential, Fourier transform infrared (FT-IR) spectra, X-ray diffraction (XRD) patterns and X-ray photoelectron spectroscopy (XPS). The mass content of Gd^{3+} in Gd^{3+}@CGO was determined by ICP-OES. In order to perform the ICP-OES test, Gd^{3+}@CGO was dispersed into deionised water to form a uniform stable dispersion with a concentration of 0.1 mg mL^{-1}. The lateral sizes and the morphologies of the GO, CGO and Gd^{3+}@CGO were undertook by a high-resolution transmission electron microscope (HRTEM, 200 kV, JEOL JEM-2100). Zeta potentials of GO, CGO and Gd^{3+}@CGO aqueous dispersion (1mg mL^{-1}, pH=7) were measured with a Nano-ZS90 Nanosizer (Malvern). FT-IR spectra with a resolution of 4cm^{-1} were recorded by a Bruker TENSOR 27 FT-IR spectrometer. XRD patterns were scanned in the range of 10-50 ^{o} at a scan rate of 1 ^{o}/min by a D8Advance X-ray diffractometer (Bruker axs Company, Germany) with Cu Kα radiation (40 kV, 20 mA, λ=1.54051 Å). XPS (K-Alpha, Thermo Scientific Company, UK) was performed using a focused monochromatic Al Kα X-ray (1486.7 eV), which was also used to identify the element composition of Gd^{3+}@CGO.

2.5. Relaxometric Measurement

The T_1-weighted image and relaxation rate r_1 of Gd^{3+}@CGO were measured, and made a comparison with clinical Magnevist MRI contrast agent with the same concentration of Gd^{3+} (0.05 mM). To measure the r_1 of the Gd^{3+}@CGO, the relaxation time (T_1) was measured using a 3.0 T MRI scanner (GE Medical Systems). T_1-weighted images were obtained with a SE sequence (TR/TE= 300 ms/20 ms, Matrix 256×256 pixel,

FOV 24 cm×24 cm, NEX 1, slice thickness of 5 mm, gap 1.5 mm). In order to acquire the T_1 values, inversion recovery sequence was used, applying three different TI (TI=100, TI=300, TI=600, TR/TE 4000 ms/9.2 ms). The r_1 is estimated based on Equation (1):[21]

$$(1/T_1)_{obsd}=(1/T_1)_{dia}+r_1\times[M]. \quad (1)$$

Where $(1/T_1)_{obsd}$ is the observed relaxation rate of water proton in the presence of paramagnetic species, $(1/T_1)_{dia}$ is the relaxation rate in the absence of the paramagnetic species and $[M]$ is the molar concentration of the paramagnetic species.

3. Results and Discussion

3.1. The formation of CGO

After treatment with chloroacetic acid under strongly alkaline conditions, GO underwent fast deoxygenations, and the π-π conjugated structure in GO was recovered. GO with a lateral size of approximately 200 nm (Fig.1a) showed a high degree of oxidation (the atom ratio of O/C is 0.43, determined by XPS, Fig.1d), which was then treated by chloroacetic acid under a strongly alkaline conditions to obtain CGO. In this case, hydroxyl groups including those derived from hydrolyzed epoxy groups and the inherent hydroxyl groups on the GO sheet were partially eliminated under the strongly alkaline conditions. Consequently, the atom ratio of O/C was reduced to 0.32 (determined by XPS, Fig.1e) in CGO, and the π-π conjugated structure was partially recovered.[22] As shown in the C1s core-level spectrum of of GO (curve 1, Fig.2a), the peaks at approximately 284.7 eV, 287 eV and 289 eV are attributed to the C-C (C=C), C-O and C=O (coming from ketone and carboxyl groups) bond, respectively. After GO was converted to CGO, the area of C-O peak was reduced, while the area of C-C (C=C) peak was increased obviously. This was in consistence with the Raman spectra, where the i(D)/i(G) belonging to CGO was lower than that of GO (Fig.S1).[23]

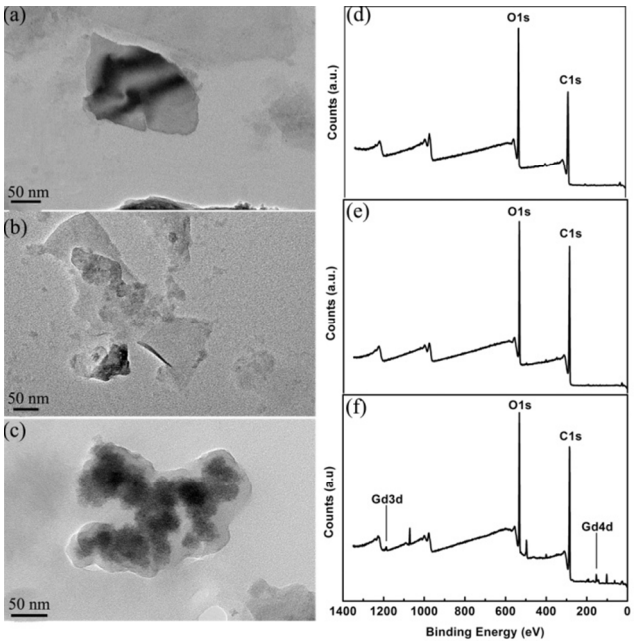

Fig.1 TEM images and corresponding wide-scan XPS spectra of GO (a, d), CGO (b, e) and Gd^{3+}@CGO (c, f).

After GO was converted to CGO, the layer distance decreased due to the restoration of the π-π conjugated structure, and the lateral size showed a little increase. The peak in the XRD pattern of GO at 2θ of 12° corresponds to a layer-to-layer distance (d-spacing) of approximately 0.73 nm,[24] while a wide diffraction peak at 2θ of 24° (corresponding to d-spacing 0.37 nm) superimposed on a broad scattering background is observed in the XRD curve of CGO (Fig.2b). The lateral size of CGO is approximately 220 nm which is slightly higher than that of GO (200 nm) (Fig.1).

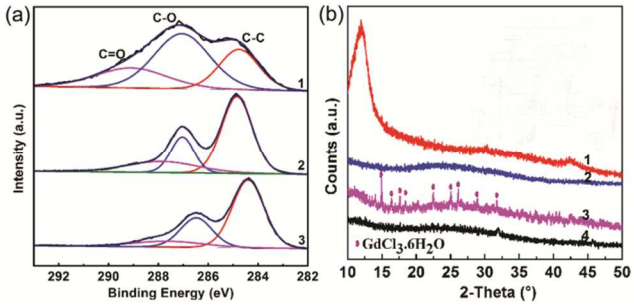

Fig.2 (a) C1s core-level XPS spectra of (1: GO; 2: CGO; 3: rGO) and (b) XRD patterns (1: GO; 2: CGO; 3: Mx; 4: Gd^{3+}@CGO)

Though a portion of epoxy groups were hydrolyzed to hydroxyl groups and further eliminated from GO sheets, quite a few epoxy and hydroxyl groups did convert into carboxyl groups during the carboxylation process of GO. In order to certify that GO was carboxyl-functionalized successfully, a control test was carried out as follows: GO was treated through the same procedure under an alkaline condition as mentioned for preparation of CGO except for adding $ClCH_2COOH$, the resulting product was named as rGO. The molar ratio of C=O to C-O bonds in CGO was determined to be approximatively 0.96:1, which was larger than that in rGO (0.48:1) or in GO (0.46:1), as demonstrated in the C1s core-level spectra (Fig.2a, Table S1). The Zeta potential of CGO aqueous solution was -50.6 mV, which was more negative in comparison with -48.2 mV of GO aqueous solution at the same concentration and pH value. This further confirmed the carboxylation of GO and implied the good dispersibility of CGO. Since it is well known that an absolute value of Zeta potential higher than 30 mV demonstrates sufficient charge repulsion to ensure a stable dispersion.

3.2. The formation of Gd^{3+}@CGO

Rather than GO and rGO, CGO with smaller interlayer spacing and more carboxyl groups can anchor many free Gd^{3+} ions stably for at least 1 year. It is noticed that CGO, GO as well as rGO dispersions still remained uniform and stable after addition of $GdCl_3.6H_2O$ solution, which had to be precipitated with saturated NaCl aqueous solution. The supernatant of each solution was collected for xylenol orange test, respectively. With one drop of xylenol orange solution added to approximately 10 mL of each supernatant, the supernatant of

the CGO solution appeared yellow, whereas the supernatant of either GO or rGO solution turned to purple. An ICP-OES test showed a particularly low concentration of Gd^{3+} (0.14 ppm) in the supernatant of CGO dispersion, which may contain a few Gd^{3+} ions that anchored on the smaller CGO sheets. So, in order to further demonstrate that few free Gd^{3+} ions existed in the CGO solution, the dialysate of the CGO dispersion was tested by ICP-OES, too. There was no Gd^{3+} ions can be detected in the dialysate until CGO dispersion was dialyzed for 24 h (0.023 ppm). Thus, we can say that the CGO can serve as a nanocarrier to anchor Gd^{3+}, whereas the GO and rGO can not! The Gd^{3+} ions were anchored extremely stably by CGO, which remained unchanged even after 1 year as demonstrated by the xylenol orange testing results (Fig. 3). Moreover, there was no free Gd^{3+} detected in the dialysate even when the CGO dispersion (after reacted with $GdCl_3.6H_2O$ for 12 h) was dialyzed against deionised water in an ultrasonic system (300W) for 1 h.

A portion of carboxyl groups in CGO were consumed through forming electrostatic interaction with Gd^{3+}, leading to intermolecular aggregation of CGO. After CGO dispersion interacted with $GdCl_3{\cdot}6H_2O$ for 12 h, pure products were collected as described in *Sec 2.3*. The pure products displayed Zeta potential of -40.6 mV which was higher than -50.6 mV of CGO when dispersed in deionised water forming a dispersion of 1 mg mL^{-1}, indicating that a portion of the carboxyl groups are consumed by electrostatic adsorption of Gd^{3+}.[17] This kind of electrostatic interaction between Gd^{3+} and CGO was further proved by the appearance of the absorption peaks belonging to the carboxylate at 1614 cm^{-1} and 1373 cm^{-1} in the FT-IR spectrum of the pure product (detailed analysis was put in the part 3 of SI, Fig.S3). In addition, the lateral size of the CGO sheet was increased from 220 nm to 260 nm after encapsulating Gd^{3+} (Fig.1b, c). The TEM image of the pure products also suggested that, Gd^{3+} ion clusters were internally-loaded in the confined space of CGO (Fig.1c).

As described above, CGO can be directly used as a nanocarrier for Gd^{3+} ion clusters without any further functionalization. The wide scan XPS spectra confirm the existence of Gd^{3+} in the pure products (Fig. 1f). And the mass concentration of Gd^{3+} in Gd^{3+}@CGO was 2.8 wt% determined by ICP-OES, which was very close to the theoretical value (3.1 wt%). This result consisting with the outcome of xylenol orange test showed that Gd^{3+} ions from $GdCl_3{\cdot}6H_2O$ were all anchored stably on CGO after they reacted with each other for 12 h. The pure products derived from CGO and $GdCl_3{\cdot}6H_2O$ were name as Gd^{3+}@CGO.

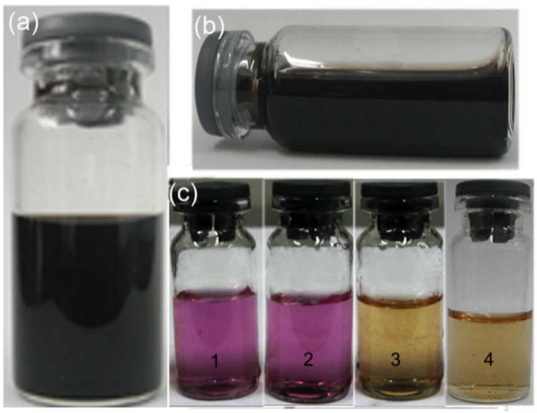

Fig.3 (a, b) Snapshots of Gd^{3+}@CGO dispersion with a concentration of 1mg mL^{-1}; (c) outcomes of xylenol orange tests (1, 2：GO, rGO solution reacted with $GdCl_3.6H_2O$ for 12 h, respectively； 3, 4: the freshly prepared Gd^{3+}@CGO dispersion, and Gd^{3+}@CGO dispersion stored for 1 year, respectively).

3.3. Relaxation properties of Gd^{3+}@CGO

The T_1 relative signal intensity of Gd^{3+}@CGO was significantly higher than that of clinical Magnovist containing the same amount of Gd^{3+}. The imaging performance of the Gd^{3+}@CGO was tested using 3.0 T MR (GE Medical Systems). It can be seen in Fig.4 that Gd^{3+}@CGO shows much brighter contrast than Magnovist, while the pristine GO and CGO do not show any bright but a little dark contrast. This indicates that the Gd^{3+} ions are anchored on CGO and show bright contrast. The dark contrast of GO and CGO is caused by the trace amounts of Mn^{2+} ions confined between their sheets.[25] The r_1 of Gd^{3+}@CGO is 63.8 mM^{-1} S^{-1} which is approximately 14 times higher compared with r_1 ~4.6 mM^{-1} S^{-1} of Magnovist in water with the same Gd^{3+} concentration ([Gd^{3+}]=0.05mM). Furthermore, both the brightness of T_1-weighted image and the r_1 value of Gd^{3+}@CGO do not show significant decrease after the Gd^{3+}@CGO is dialyzed against deionised water through a 500D dialysis bag with ultrasonic treatment (300W) for 1 h. The r_1 of Gd^{3+}@CGO dialyzed against deionised water is 54.1 mM^{-1} S^{-1}. This further demonstrated that the Gd^{3+} ions are encapsulated in CGO sheets stably. Herein, the slightly reduced r_1 value of 54.1 mM^{-1} S^{-1} may be caused by a small decrease of Gd^{3+} concentration after dialysis. During the dialysis of Gd^{3+}@CGO solution, impurities (e.g. MnO_2, NaOH) originated from GO and CGO preparation procedures penetrate into the dialysate, while the water molecular pass into the Gd^{3+}@CGO solution, which finally leading to Gd^{3+} content in the dialyzed Gd^{3+}@CGO solution is little lower than 0.05 mM.

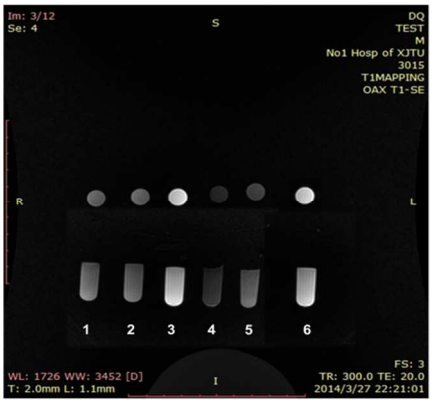

Fig.4 T_1W_I reference images (1: H_2O; 2: Magnovist; 3: Gd^{3+}@CGO; 4: GO; 5: CGO; 6: Gd^{3+}@CGO after dialysis against deionised water for 1h with assistance of ultrasonic vibration).

The significantly enhanced longitudinal relaxivity of Gd^{3+}@CGO can be attributed to its aggregation behavior and the efficient access of Gd^{3+} ion cluster to water molecules. It has been reported that either the accessibility of Gd^{3+} centers to water molecules or the intermolecular aggregation of MRI contrast agents plays an important role in the r_1 enhancement of gadonanotube or gadofullerene MRI contrasts.[11, 12] As demonstrated by TEM images, Gd^{3+}@CGO did undergo slightly aggregation in comparison with the original CGO. Furthermore, the rich hydrophilic groups (-COOH, -OH) on the CGO surface are expected to improve the proton conductivity, thus promotes access of Gd^{3+}-ion clusters centers in Gd^{3+}@CGO to water molecules.[26]

The truth that Gd^{3+} ions are anchored stably on CGO showing few toxicity against HeLa cells, suggests low cytotoxicity of Gd^{3+}@CGO. According to the CCK-8 assay, we found out that CGO had few negative impacts on the viability of HeLa cells though GO did produce a few negative impacts. We attributed this phenomenon to better water dispersibility of CGO than GO. The viability of HeLa cells are reduced to lower than 80 % when incubated with a concentration of GO higher than 80 μg mL^{-1}, while remain more than 80 % when incubated in such a high concentration of CGO of 200 μg mL^{-1} for 24 h (Fig.S3, testing method is shown in the part 4 of SI). Since in Gd^{3+}@CGO, Gd^{3+} ions are stably anchored on CGO, we think that Gd^{3+}@CGO will not have significant negative impacts on cell viability. The cytotoxicity study of Gd^{3+}@CGO has been in progressing. All in all, Gd^{3+}@CGO easily prepared in our work, which exhibit particularly high r_1 value and possess potential biocompatibility, is an attractive candidate for high-performance MRI imaging agents.

3.4. Possible mechanism for the interaction between Gd^{3+} and CGO

The present analysis results do not show direct evidence for the formation of coordination bonds between Gd^{3+} and carboxyl groups of CGO. XPS has been widely used to detect the formation of complexes according to the fact that the binding energy will increase for the ligand atom and decrease for the central atom after forming a complex.[27] The XPS analysis of Gd^{3+}@CGO indicates that there is no detectable coordination bond between the carboxyl groups in CGO and the Gd^{3+}. For instance, the gadolinium in Gd^{3+}@CGO appears to play a role of central atom, whose binding energies reduce slightly to 143.0 eV, 148.7 eV and 1187.4 eV from 143.2 eV, 149.1 eV and 1187.7 eV (corresponding to $Gd4d_{5/2}$, $Gd4d_{3/2}$ and Gd3d, respectively [28]) in Mx. However, the oxygen atoms belonging to Gd^{3+}@CGO do not perform as ligand atoms, whose binding energies do not increase compared with that in CGO (Fig.5). It is reported in Ref.18 that Gd^{3+} can be chelated by the carboxyl groups in GO functionalized with *p*-carboxyphenyldiazonium salt, but the coordination interaction was illustrated without any direct experimental evidence (spectral data). In addition, although there are several kinds of metal ions (e.g. Ca^{2+}, Mg^{2+}, Eu^{3+}) have been shown to be chelated by oxygen-containing functional groups on the GO sheets,[16, 29] it is a well known fact that Gd^{3+} is difficult to be chelated due to its large radius. Thus, the question of whether Gd^{3+} can be chelated by the carboxyl groups in CGO still remains.

As for our point of view, since no apparent coordination bonds are detected, besides the electrostatic adsorption effect, the encapsulation effects may play a key role in stably anchoring Gd^{3+} on CGO for up to 1 year, similar to the case that Gd^{3+} is encapsulated in carbon nanotubes and fullerenes. The TEM image of Gd^{3+}@CGO has shown the internally-loaded of Gd^{3+} in CGO hereinbefore. The XRD pattern of Gd^{3+}@CGO also gives us a suggestion from another hand. There are no obvious diffraction peaks attributed to $GdCl_3{\cdot}6H_2O$ in the XRD pattern of Gd^{3+}@CGO. According to Ref. 12, the absence of XRD diffraction patterns belonging to $GdCl_3{\cdot}6H_2O$ in gadonanotubes was attributed to the low Gd^{3+} content. However, we found that rather than the low Gd^{3+} content, the encapsulation effect of CGO may be the main cause for the absence of the XRD diffraction pattern of $GdCl_3{\cdot}6H_2O$ in Gd^{3+}@CGO, because obvious diffraction peaks assigned to $GdCl_3{\cdot}6H_2O$ appeared in XRD curve of Mx containing the same mass content of Gd^{3+} as those in Gd^{3+}@CGO.

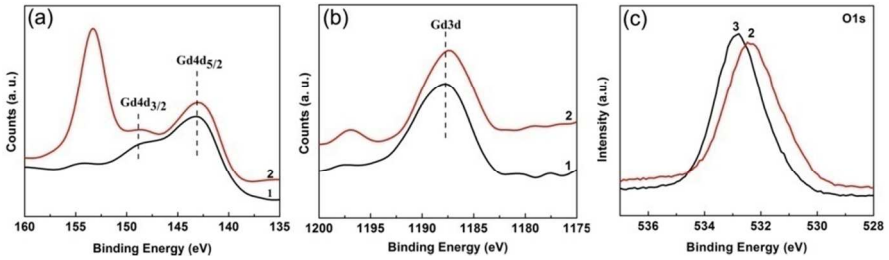

Fig.5 (a) Gd4d and (b) Gd3d core-level XPS spectra (1: Mx; 2: Gd^{3+}@CGO), as well as (c) O1s core-level XPS spectra (2: Gd^{3+}@CGO; 3: CGO)

In summary, though it has been shown that a certain amount of Gd^{3+} can be stably anchored on the CGO, the mechanism still need further investigation. Several questions needed to be answered in our future work. For instance, do the oxygen containing groups (especially carboxyl groups) in CGO form coordination complexes with Gd^{3+}? Is there any other interaction besides the electrostatic and encapsulation effects which contributes to anchoring the Gd^{3+}?

4. Conclusions

An easy synthetic strategy which leads to a high performance MRI contrast agent, named Gd^{3+}@CGO, is developed using CGO as a nanocarrier. Differing from the conventional carriers which must rely on polydentate ligands, CGO can anchor Gd^{3+} directly and stably. In addition, CGO with intrinsic high hydrophilic property guarantees the accessibility of Gd^{3+} centers to water molecules and high r_1 value of Gd^{3+}@CGO. The Gd^{3+}@CGO possesses the capability of casting a bright T_1-weighted image with r_1 ~63.8 mM^{-1} S^{-1}, which is nearly 14 times as the present clinically used Magnevist. In addition, the few cytotoxicity of CGO indicates the potential biocompatibility of Gd^{3+}@CGO. Although the load mechanism is not yet clear, it is exciting to find that Gd^{3+} ion clusters encapsulated in CGO remained stable at least 1 year, implying that CGO has the ability to absorb other metals.

Acknowledgements

This work is supported by the National Natural Science Foundation of China (no. 81171318) and Shaanxi Health Department Foundation, China (no. 2010E07).

Notes and references

[a] *Department of Applied Chemistry, School of Science, Xi'an Jiaotong University, Xi'an, 710049, China. Fax: +86 29 83237910; Tel.: +86 29 68640809;*

E-mail: rgfp-jing@mail.xjtu.edu.cn, yuli2012@mail.xjtu.edu.cn.

[b] *State Key Laboratory Cultivation Base for Nonmetal Composite and Functional Material, School of Materials Science and Engineering, Southwest University of Science and Technology, Mianyang, 621010, China.*

[c] *First Affiliated Hospital of Xi'an Jiaotong University, Xi'an, 710049, China.*

† Electronic Supplementary Information (ESI) available. See DOI: 10.1039/b000000x/

1. S. Srivastava, R. Awasthi, D. Tripathi, M. K. Rai, V. Agarwal, V. Agrawal, N. S. Gajbhiye and R. K. Gupta, *Small*, 2012, 8, 1099-1109.
2. X. Wang, Y. Feng, T. Ke, M. Schabel and Z.-R. Lu, *Phar. Res.*, 2005, 22, 596-602.
3. V. S. Talanov, C. A. Regino, H. Kobayashi, M. Bernardo, P. L. Choyke and M. W. Brechbiel, *Nano Lett*, 2006, 6, 1459-1463.
4. W. J. Mulder, R. Koole, R. J. Brandwijk, G. Storm, P. T. Chin, G. J. Strijkers, C. de Mello Donegá, K. Nicolay and A. W. Griffioen, *Nano Lett.* 2006, 6, 1-6.
5. F. Carniato, L. Tei, A. Arrais, L. Marchese and M. Botta, *Chem. Eur. J.* 2013, 19, 1421-1428.
6. J. S. Kim, W. J. Rieter, K. M. Taylor, H. An, W. Lin and W. Lin, *J. Am. Chem. Soc.*, 2007, 129, 8962-8963.
7. T. Akasaka, S. Nagase, K. Kobayashi, T. Suzuki, T. Kato, K. Yamamoto, H. Funasaka and T. Takahashi, *J. Chem. Soc., Chem. Commun.*, 1995, 1343-1344.
8. Y. Kubozono, H. Maeda, Y. Takabayashi, K. Hiraoka, T. Nakai, S. Kashino, S. Emura, S. Ukita and T. Sogabe, *J. Am. Chem. Soc.*, 1996, 118, 6998-6999.
9. R. D. Bolskar, A. F. Benedetto, L. O. Husebo, R. E. Price, E. F. Jackson, S. Wallace, L. J. Wilson and J. M. Alford, *J. Am. Chem. Soc.*, 2003, 125, 5471-5478.
10. P. P. Fatouros, F. D. Corwin, Z.-J. Chen, W. C. Broaddus, J. L. Tatum, B. Kettenmann, Z. Ge, H. W. Gibson, J. L. Russ and A. P. Leonard, *Radiology*, 2006, 240, 756-764.
11. E. Y. Zhang, C. Y. Shu, L. Feng and C.-R. Wang, *J. Phys. Chem. B*, 2007, 111, 14223-14226.
12. B. Sitharaman, K. R. Kissell, K. B. Hartman, L. A. Tran, A. Baikalov, I. Rusakova, Y. Sun, H. A. Khant, S. J. Ludtke and W. Chiu, *Chem. Commun.*, 2005, 3915-3917.
13. Y. Sheng, X. S. Tang, E. W. Peng and J. M. Xue, *J. Mat. Chem. B*, 2013, 1, 512-521.
14. S. Sun and P. Wu, *J. Mat. Chem.*, 2011, 21, 4095-4097.
15. L. Zhang, J. Xia, Q. Zhao, L. Liu and Z. Zhang, *Small*, 2009, 6, 537-544.
16. S. Park, K.-S. Lee, G. Bozoklu, W. Cai, S. T. Nguyen and R. S. Ruoff, *ACS nano*, 2008, 2, 572-578.
17. A. J. Shen, D. L. Li, X. J. Cai, C. Y. Dong, H. Q. Dong, H. Y. Wen, G. H. Dai, P. J. Wang and Y. Y. Li, *J. Biomed. Mater. Res. Part A*, 2012, 100A, 2499-2506.
18. A. Gizzatov, V. Keshishian, A. Guven, A. M. Dimiev, F. Qu, R. Muthupillai, P. Decuzzi, R. G. Bryant, J. M. Tour and L. J. Wilson, *Nanoscale*, 2014.
19. H. Yue, W. Wei, Z. Yue, B. Wang, N. Luo, Y. Gao, D. Ma, G. Ma and Z. Su, *Biomaterials*, 2012.
20. L. Zhang, J. Liang, Y. Huang, Y. Ma, Y. Wang and Y. Chen, *Carbon*, 2009, 47, 3365-3368.
21. S. Setua, D. Menon, A. Asok, S. Nair and M. Koyakutty, *Biomaterials*, 2010, 31, 714-729.
22. X. Fan, W. Peng, Y. Li, X. Li, S. Wang, G. Zhang and F. Zhang, *Adv. Mater.*, 2008, 20, 4490-4493.
23. A. C. Ferrari and D. M. Basko, *Nature nanotechnology*, 2013, 8, 235-246.
24. D. A. Dikin, S. Stankovich, E. J. Zimney, R. D. Piner, G. H. Dommett, G. Evmenenko, S. T. Nguyen and R. S. Ruoff, *Nature*, 2007, 448, 457-460.
25. B. S. Paratala, B. D. Jacobson, S. Kanakia, L. D. Francis and B. Sitharaman, *PloS one*, 2012, 7, e38185.
26. A. Enotiadis, K. Angjeli, N. Baldino, I. Nicotera and D. Gournis, *Small*, 2012, 8, 3338-3349.

27. F. Mercier, C. Alliot, L. Bion, N. Thromat and P. Toulhoat, *J. Eelectron. Spectrosc. Relat. Phenom.*, 2006, 150, 21-26.
28. D. Raiser and J. Deville, *J. Eelectron. Spectrosc. Relat. Phenom.*, 1991, 57, 91-97.
29. J. Y. Kim, J. B. Lee, H. J. Kim, K. Shin, Y. S. Yu and Y. Oh, *Bull. Korean Chem. Soc.*, 2010, 31, 1485-1488.